Thermochimica Acta, 78 (1984) 449–454
Elsevier Science Publishers B.V., Amsterdam – Printed in The Netherlands

Note

THERMAL STUDY OF RARE-EARTH TRIFLUOROACETATE COMPLEXES WITH THIOXANE-OXIDE

P.O. DUNSTAN

Instituto de Química, Universidade Estadual de Campinas, C.P. 6154, CEP 13100, Campinas, São Paulo (Brazil)

G. VICENTINI and L.B. ZINNER

Instituto de Química, Universidade de São Paulo, C.P. 20.780, CEP 01498, São Paulo (Brazil)

(Received 9 March 1984)

This note describes the thermal study of the complexes of general formula $[Ln(F_3C{-}COO)_3(TSO)_3]$ (Ln = La–Lu, Y; TSO = thioxane-oxide), using TG and DSC techniques.

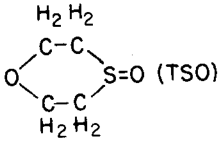

EXPERIMENTAL

The compounds were prepared by reaction of the hydrated lanthanide salts with warm TSO, followed by the addition of 2,2-dimethoxypropane [1]. The isolated complexes were washed with 2,2-dimethoxypropane and dried in vacuo over anhydrous calcium chloride. Carbon and hydrogen analysis were performed in a Perkin-Elmer microanalyser (model 240). The determination of the metal ions was carried out by complexometric titration with EDTA [2]. The TG studies were made in nitrogen atmosphere in a Perkin-Elmer TGS-1 system, using samples varying in weight from 0.798 to 1.000 mg and a heating rate of 10°C min^{-1}. The DSC curves were recorded in nitrogen atmosphere using a Perkin-Elmer DSC-2 equipment at a heating rate of 40 K min^{-1} in the 340–660 K temperature range.

RESULTS AND DISCUSSION

The compounds of general formula $[Ln(F_3C{-}COO)_3(TSO)_3]$ (Ln = La–Lu, Y; TSO = thioxane-oxide) behave as non-electrolytes in nitromethane and acetonitrile.

A comparison of the X-ray powder patterns indicates that they form only one isomorphous series. IR spectra suggest the existence of two types of coordination of the anion to the central ion and that TSO is bonded through the sulfoxide oxygen. Emission spectra of the europium compound indicate a D_{2d} symmetry for the complex species [1].

Figure 1 contains the TG and Fig. 2 the DSC curves obtained for all the complexes. Table 1 presents the thermoanalytical data, together with the apparent melting points.

The thermal processes of decomposition of the compounds can be represented by the following sets of equations

(a) $$[\mathrm{Ln(F_3C{-}COO)_3(TSO)_3}] \rightarrow [\mathrm{Ln(CF_3C{-}COO)_3TSO}] + 2\,\mathrm{TSO} \qquad (1)$$

$$[\mathrm{Ln(F_3C{-}COO)_3TSO}] \rightarrow \mathrm{LnF_3} + \mathrm{TSO} + \text{gaseous products} \qquad (2)$$

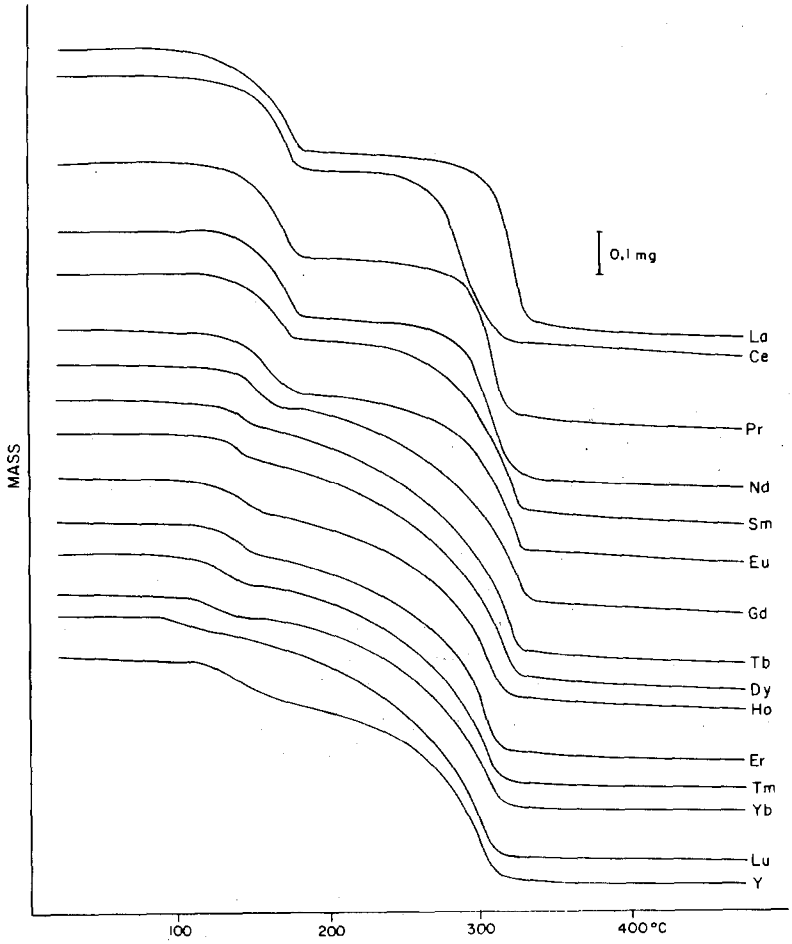

Fig. 1. TG curves for the compounds of formula $[\mathrm{Ln(F_3C{-}COO)_3(TSO)_3}]$.

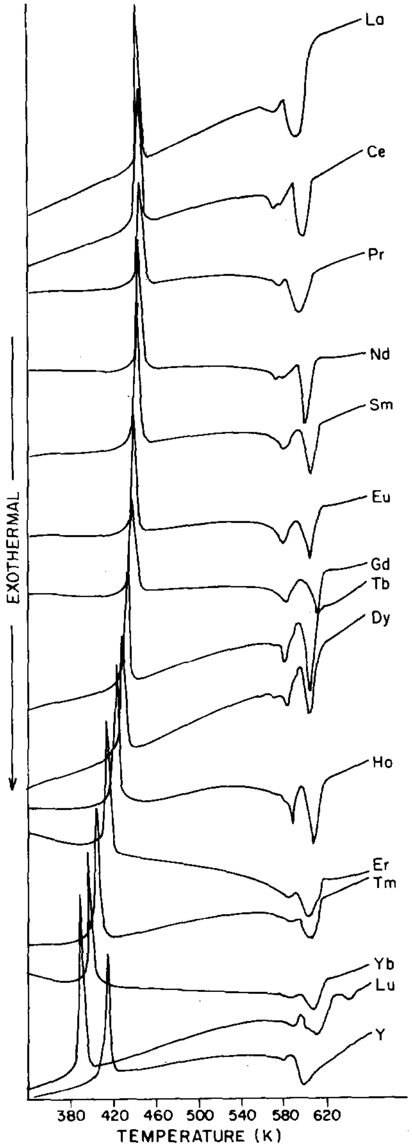

Fig. 2. DSC curves for the compounds of formula $[\mathrm{Ln(F_3C{-}COO)_3(TSO)_3}]$.

$$\text{(b)}\quad [\mathrm{Ln(F_3C{-}COO)_3(TSO)_3}] \rightarrow [\mathrm{Ln(F_3C{-}COO)_3(TSO)_{1.5}}] + 1.5\ \mathrm{TSO} \qquad (3)$$

$$[\mathrm{Ln(F_3C{-}COO)_3(TSO)_{1.5}}] \rightarrow \mathrm{LnF_3} + 1.5\mathrm{TSO} + \text{gaseous products} \qquad (4)$$

$$\text{(c)}\quad [\mathrm{Ln(F_3C{-}COO)_3(TSO)_3}] \rightarrow [\mathrm{Ln(F_3C{-}COO)_3(TSO)_{0.5}}] + 2.5\ \mathrm{TSO} \qquad (5)$$

$$[\mathrm{Ln(F_3C{-}COO)_3(TSO)_{0.5}}] \rightarrow \mathrm{LnF_3} + 0.5\mathrm{TSO} + \text{gaseous products} \qquad (6)$$

$$\text{(d)}\quad [\mathrm{Ln(F_3C{-}COO)_3(TSO)_3}] \rightarrow \mathrm{Ln(CF_3COO)_3} + 3\ \mathrm{TSO} \qquad (7)$$

$$\mathrm{Ln(F_3C{-}COO)_3} \rightarrow \mathrm{LnF_3} + \text{gaseous products} \qquad (8)$$

TABLE 1

Thermoanalytical data of the compounds of formula [$Ln(CF_3COO)_3 \cdot (TSO)_3$]

Process	Apparent melting point (°C)	Weight loss (%)		Temperature range (°C)	Peak temperature (°C) DSC	Enthalpy (kJ mol^{-1})
residue		Calc.	Obs.			
(1)	180	29.96	28.0	156–187	175	62.5
(2)		47.12	45.7	303–323	309	−45.7
					327	−59.4
LaF_3		$\overline{23.36}$	$\overline{23.0}$	323–500	–	–
(1)	180	28.62	26.1	158–187	175	65.1
(2)		47.90	49.7	264–303	303	−66.2
					331	−56.1
CeF_3		$\overline{23.47}$	$\overline{23.6}$	303–500	–	–
(1)	175	28.60	28.6	161–187	175	60.9
(2)		47.86	44.6	289–315	309	−19.1
					329	−57.4
PrF_3		$\overline{23.54}$	$\overline{23.2}$	315–500	–	–
(1)	175	28.48	25.9	162–188	174	50.6
(2)		47.67	45.1	289–318	305	−31.8
					333	−54.9
NdF_3		$\overline{23.84}$	$\overline{24.5}$	318–500	–	–
(3)	173	21.21	20.9	155–184	171	71.4
(4)		54.40	51.6	285–336	311	−34.0
					337	−47.6
SmF_3		$\overline{24.39}$	$\overline{24.5}$	336–500	–	–
(3)	157	21.17	22.6	148–186	169	67.4
(4)		54.30	50.4	241–327	311	−33.7
					336	−50.6
EuF_3		$\overline{24.53}$	$\overline{24.2}$	327–500	–	–
(5)	154	35.07	33.1	147–295	163	64.4
(6)		39.93	38.2	295–331	312	−27.1
					342	−50.9
GdF_3		$\overline{25.00}$	$\overline{25.3}$	331–500	–	–
(1)	145	28.00	27.8	141–278	159	61.4
(2)		46.85	44.2	278–326	312	−39.2
					336	−57.5
TbF_3		$\overline{25.15}$	$\overline{26.5}$	326–500	–	–
(5)	150	34.85	35.3	141–288	153	65.0
(6)		39.69	39.7	288–326	313	−59.6
					335	−66.8
DyF_3		$\overline{25.46}$	$\overline{25.9}$	326–500	–	–
(7)	142	41.70	40.8	133–289	148	71.9
(8)		32.63	35.2	289–317	318	−37.3
					337	−52.9
HoF_3		$\overline{25.67}$	$\overline{24.2}$	317–500	–	–

TABLE 1 (continued)

Process residue	Apparent melting point (°C)	Weight loss (%)		Temperature range (°C)	Peak temperature (°C) DSC	Enthalpy (kJ mol^{-1})
		Calc.	Obs.			
(7)	143	41.59	38.3	123–292	139	67.8
(8)		32.53	35.0	292–313	314	−50.5
					334	−50.5
ErF_3		$\overline{25.88}$	$\overline{26.1}$	313–500	–	–
(7)	132	41.52	40.4	123–292	130	70.6
(8)		32.48	30.0	292–313	315	−30.3
					333	−47.1
TmF_3		$\overline{26.01}$	$\overline{26.1}$	313–500	–	–
(5)	125	34.42	33.3	122–296	122	70.8
(6)		39.20	38.2	296–317	316	−9.8
					335	−54.1
YbF_3		$\overline{26.36}$	$\overline{26.5}$	317–500	–	–
(7)	118	41.22	43.9	114–298	115	78.7
(8)		32.25	29.0	298–321	317	−41.3
					338	−77.0
LuF_3		$\overline{26.53}$	$\overline{26.1}$	321–500	–	–
(7)	145	45.72	44.8	134–291	142	57.6
(8)		35.77	34.3	291–313	311	−4.7
					331	−62.9
YF_3		$\overline{18.51}$	$\overline{18.5}$	313–500	–	–

According to Rillings and Roberts [3] the volatile decomposition products may consist of CO, CO_2, COF_2, $F_3C{-}COF$ and $(F_3C{-}CO)_2O$.

The final residues are, according to TG data (Table 1), the respective lanthanide fluorides, and this result can be extended to the whole series. It is interesting to consider that experiments simulating the TG condition, but using large amounts of material, give residues that contain appreciable amounts of fluorides, as observed by glass corrosion tests, by heating with concentrated sulfuric acid. The compounds from lanthanum to samarium decompose in two steps. The remainder of the curves are toboggan type. Partial or total elimination of TSO is observed, followed by decomposition with evolution of several gaseous products [3]. For the heavier lanthanides it is obvious that the evolution occurs more easily.

The DSC curves, consistent with TG data, present in all cases an endothermic peak that corresponds to the melting of the compounds and the evolution of TSO. It is clear from Fig. 3, in which is depicted the variation of the apparent melting points and DSC peaks are shown as a function of the ionic radii, that the position of this peak depends on the decreasing lanthanide radii. The compound of yttrium, with an ionic radius similar to that of erbium, presents a peak in practically the same region, the shape of the curve

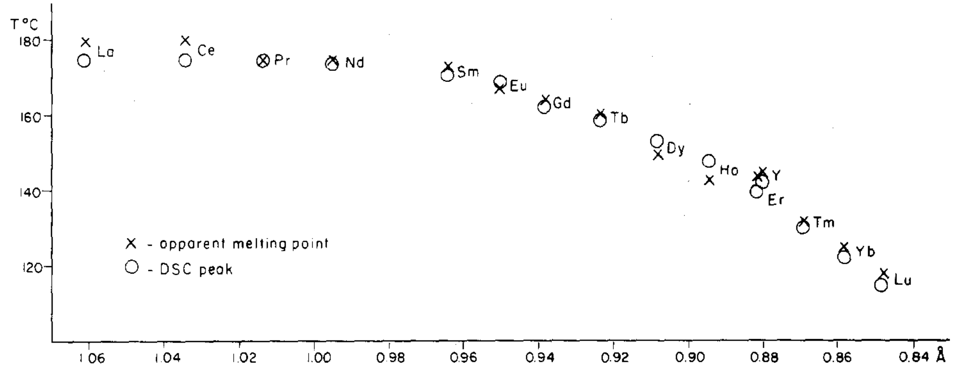

Fig. 3. Apparent melting points and DSC peaks versus trivalent ionic radii.

(Fig. 2) also being similar. A "gadolinium break" may also be observed. At higher temperatures at least two exothermic peaks are observed, corresponding to decomposition of the trifluoroacetate. The positive and negative enthalpies together with peak temperature of such transformations are also presented in Table 1.

ACKNOWLEDGMENT

The authors are much indebted to CNPq for financial support.

REFERENCES

1 L.B. Zinner, Anais do VI Simpósio Anual da Academia de Ciências do Estado de São Paulo, 1 (1982) 185.
2 S.J. Lyle and M.Md. Rahman, Talanta, 10 (1973) 1177.
3 K.W. Rillings and J.E. Roberts, Thermochim. Acta, 10 (1974) 285.